A comparative thermodynamic analysis of helium distribution systems with central and distributed precooling heat exchangers

IOP Conf. Series: Materials Science and Engineering **502** (2019) 012173 doi:10.1088/1757-899X/502/1/012173

A comparative thermodynamic analysis of helium distribution systems with central and distributed precooling heat exchangers

J Fydrych[1] and S Pietrowicz[2]

[1] European Spallation Source ERIC, P.O. Box 176, 22 100 Lund, Sweden
[2] Wroclaw University of Science and Technology, Department of Thermodynamics, Theory of Machines and Thermal Systems, Wyb. Wyspianskiego 27, 50-370 Wroclaw, Poland

jaroslaw.fydrych@esss.se

Abstract. All the cryogenic systems of large scientific facilities using He II technologies apply the Joule-Thomson expansion for final production of superfluid helium. Their cryogenic plants supply subcooled liquid helium at 4.5 K which is precooled to 2.2 K before throttling to a sub-atmospheric pressure in Joule-Thomson valves. The precooling of the 4.5 K helium can be done in one central heat exchanger or in a number of small heat exchangers located just at the throttling valves. Since there are cons and pros for the both architectures, it is important to take into account all thermodynamics and financial aspects in choosing the best layout in the preliminary design of any new large He II system.
The paper presents a comparative thermodynamic analysis of the both cooling schemes in respect to the size of cryogenic distribution systems and heat loads subjected to their components. The analysis is based on calculations of the second-law efficiencies which are preceded by a numerical modelling of temperature and pressure distributions along the process lines.

1. Introduction

All the cryogenic systems of large scientific facilities using superfluid helium technologies apply the Joule-Thomson expansion for final production of the superfluid helium. Usually their cryogenic plants supply subcooled liquid helium at 4.5 K and around 3 bar(a), which is commonly called supercritical helium. The 4.5 K helium is precooled to a temperature of 2.2 K before throttling to a sub-atmospheric pressure of 16 to 41 mbar in the Joule-Thomson valves in order to produce superfluid helium at a temperature of 1.8 K to 2.1 K. The precooling of the 4.5 K helium is performed either at the throttling valves or somewhere between the cryoplant and 2 K helium users. The first solution is schematically presented in Figure 1 and the other is shown in Figure 2. The design with distributed heat exchanges can be found in the cryogenic distribution systems of LHC [1], SNS [2], ESS [3] and PIP-II [4], whilst the layout with a central heat exchanger is used in the XFEL and LCLS-II cryogenic systems [5 and 6]. In both cases the systems have a thermal shield at a temperature range of 40 K to 80 K. In this paper the circuit is called the high temperature thermal shield (HTTS). The system with a central heat exchanger however is equipped with an additional thermal shield at a temperature range of 5 K to 8 K, which is named here as the low temperature thermal shield (LTTS).

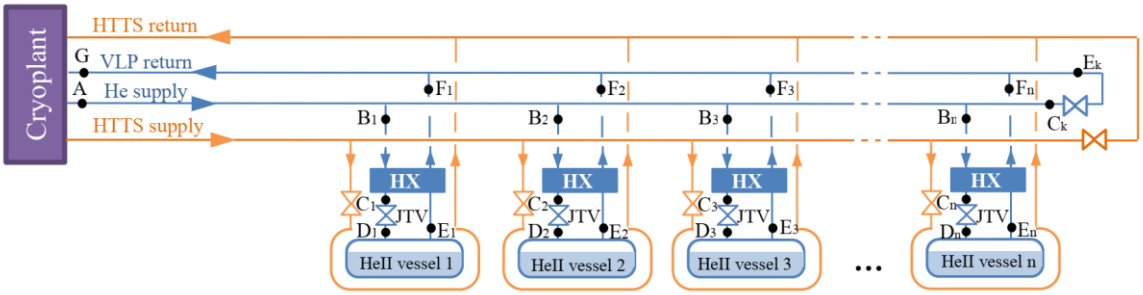

Figure 1. Schematic layout of a cryogenic distribution system with distributed precooling heat exchangers (Layout 1)

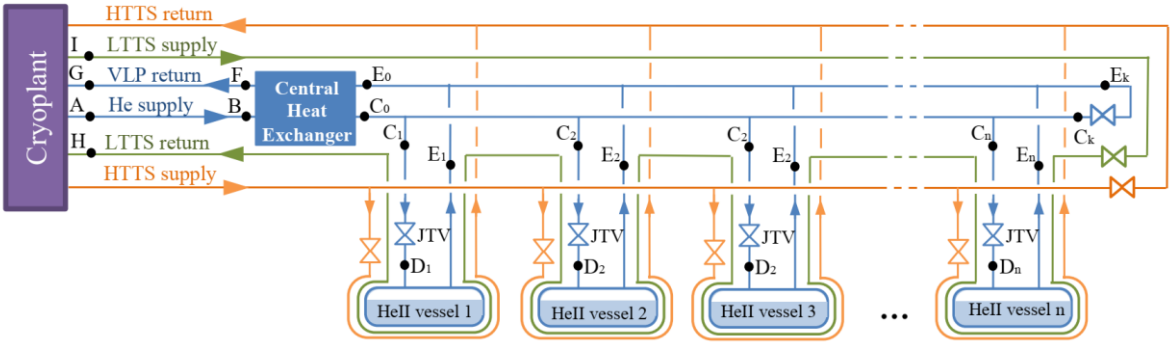

Figure 2. Schematic layout of a cryogenic distribution system with a central heat exchanger and a low temperature thermal shield circuit (Layout 2)

The paper presents a comparative thermodynamic analysis of the both types of cooling schemes, here called Layout 1 and Layout 2, in respect to the size of cryogenic distribution systems (number of cryomodules (CMs), length and sizes of process pipes) and heat loads subjected to their components.

2. Thermodynamic modelling and assumptions

The presented thermodynamic analysis is based on calculations of the exergy efficiency η_{ex} (the second-law efficiency), which is the ratio of potential useful exergy output (Ex_{net}) to potential useful exergy input (Ex_{in}). Ex_{net} represents the minimum amount of mechanical work needed for extraction of heat Q from the system. Usually an exergy flow analysis is suitable for identifying sources of irreversibilities in a thermodynamic system. For example, it was applied for the HERA cryogenic plant [7] and the LHC cryogenic distribution system [8]. Here, the exergy efficiency is used as a measure of the thermodynamic performance of the analyzed cryogenic distribution layouts that shows their capabilities to preserve the maximum available work of the process fluids.

For non-isothermal cooling processes, the Ex_{net} for steady state conditions is [8]

$$Ex_{\mathrm{net}} = Q\left(1 - \left(\frac{T_0}{T_{\mathrm{out}} - T_{\mathrm{in}}}\right) ln\left(\frac{T_{\mathrm{out}}}{T_{\mathrm{in}}}\right)\right), \tag{1}$$

where T_0 is the ambient temperature (290 K), and T_{out} and T_{in} are temperatures at the outlet and inlet of the analyzed system or subsystem, respectively. Ex_{in} represents real exergy loss [8]. For steady state processes the exergy loss is a function of flow rate $\dot{m}$, enthalpy increase Δh and entropy increase Δs:

$$Ex_{\mathrm{in}} = \dot{m}(\Delta h - T_0 \Delta s) = \dot{m}\big((h(T_{\mathrm{out}}, p_{\mathrm{out}}) - h(T_{\mathrm{in}}, p_{\mathrm{in}}) - T_0(s(T_{\mathrm{out}}, p_{\mathrm{out}}) - s(T_{\mathrm{in}}, p_{\mathrm{in}})\big)\,. \tag{2}$$

Thus, the exergy efficiency for steady thermal processes is:

$$\eta_{\mathrm{ex}} = \frac{Ex_{\mathrm{net}}}{Ex_{\mathrm{in}}} = \frac{\mathrm{Q}\left(1-\left(\frac{T_0}{T_{\mathrm{out}}-T_{\mathrm{in}}}\right)ln\left(\frac{T_{\mathrm{out}}}{T_{\mathrm{in}}}\right)\right)}{\dot{m}\left((h(T_{\mathrm{out}},p_{\mathrm{out}})-h(T_{\mathrm{in}},p_{\mathrm{in}})-T_0(s(T_{\mathrm{out}},p_{\mathrm{out}})-s(T_{\mathrm{in}},p_{\mathrm{in}})\right)}. \quad (3)$$

Pressure drops between characteristic points (see Figures 1 and 2) are calculated from the Darcy–Weisbach equation, whilst in the central and distributed heat exchanges pressure drops are assumed as equal to 3 mbar and 1 mbar, respectively. Both layouts were analyzed for 3 different geometrical configurations. Their geometrical parameters are given in Table 1. In addition, there is a 100 m transfer line connecting the distribution system with the cryoplant. The central heat exchanger in Layout 2 is located after the transfer line. The 3 configurations were exposed to 3 different heat load cases described in Table 2.

Table 1. Configurations of the distribution systems' geometries

Layout	Confi-guration	# of CMs	He supply line	VLP line	LTTS lines	HTTS lines	LTTS	HTTS in CDS	HTTS in CM
Layout 1 with distributed heat exchangers	Config. 1	30	DN50 60.3x2.3	DN150, 168.3x2.8	n/a	DN40, 48.3x2.0	n/a	⌀ 0.40m	30 m^2 per CM
	Config. 2	50	DN65 76.1x2.3	DN200, 219.1x2.8	n/a	DN50, 60.3x2.3	n/a	⌀ 0.45m	
	Config. 3	100	DN100, 114.3x2.6	DN300, 323.9x4	n/a	DN80, 88.9x2.6	n/a	⌀ 0.55m	
Layout 2 with a central heat exchanger	Config. 1	30	DN40 48.3x2.0	DN100, 114.3x2.6	DN25, 33.4x1.65	DN40, 48.3x2.0	⌀ 0.50m	⌀ 0.60m	n/a
	Config. 2	50	DN50 60.3x2.3	DN150, 168.3x2.8	DN32, 42.2x1.65	DN50, 60.3x2.3	⌀ 0.55m	⌀ 0.65m	
	Config. 3	100	DN80 88.9x2.6	DN250, 273x3.0	DN50, 60.3x2.3	DN80, 88.9x2.6	⌀ 0.65m	⌀ 0.75m	

Table 2. Heat load cases

Heat load case	Cryogenic distribution system					Dynamic heat load to cavities
	300K to 50 K	50K to 5-8 K	50K to 4.5 K	50K to 2K	5-8 K - 2K	
HL 1	3.8 W/m^2	1.0 W/m^2	1.1 W/m^2	1.2 W/m^2	0.3 W/m^2	1.0 W/m
HL 2						2.0 W/m
HL 3						3.0 W/m

Calculations of thermodynamic variables in all characteristic points of the analyzed systems were performed in a developed numerical code using the modified Richardson iteration method with a convergence error below 10^{-3}. Helium properties were taken from HePak 3.4. The temperatures and pressures in the inlets to the Helium, LTTS and HTTS supply lines at the interface between the transfer line and cryoplant are {4.5 K, 3 bara}, {5 K, 3.5 bara} and {50 K, 19.5 bara}, respectively.

3. Results and discussion

The analysis gave 18 sets of results including temperature and pressure profiles along process pipes as well as the distributions of JT expansion effectiveness, mass flow rate, and CMs' exergetic efficiency. Some examples of the results for Configuration 1 and HL3 are shown in Figures 3, 4 and 5. Temperature in the He supply line rises gradually by 0.7 K, whilst pressure drops insignificantly, due to a large diameter, which is oversized for nominal (cold) conditions in order to allow for reasonably fast cool down rates. In the VLP line the temperature increases by 1.12 K in Layout 1. Initially, at the last CMs, the increase rate is strong but later it gets suppressed by inflows of very cold helium vapor from the CM He II vessels. In Layout 2 the temperature in the He supply line drops to 2.2 K in central heat exchanger and later rises along the line by 0.36 K only, due to much smaller heat loads (LTTS effect). In the VLP

line the helium temperature rises along the line from 2.0 K to 2.17 K, and later it jumps in the central heat exchanger and transfer line to reach 3.37 K in the inlet to the cryoplant. Pressure drops in the VLP line are small but significant in respect to the allowable value of a few mbar. The helium mass flow rates in cryomodules are not constant. They continuously increase along the distribution system because of higher temperatures of the helium along the He supply line. This results in higher temperatures downstream the heat exchangers and in consequence in lower efficiencies of the Joule-Thomson expansion. The exergetic efficiency of CMs in Layout 1 varies from 43% to 32%, whilst in Layout 2 it is about twice higher (86% to 76%). The difference results from lack of the 4.5K-2.2K heat exchange process in the CMs of the second layout.

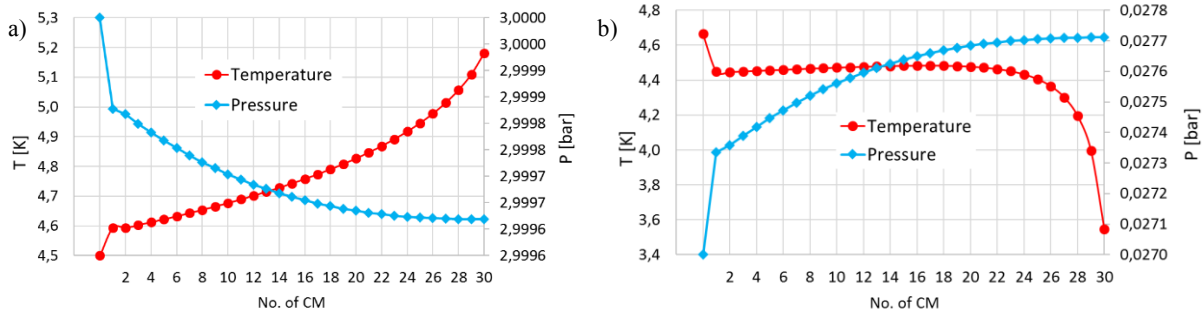

Figure 3. Distributions of temperature, pressure along the He supply (a) and VLP return (b) lines for Layout 1 in Configuration 1 and subjected to HL3

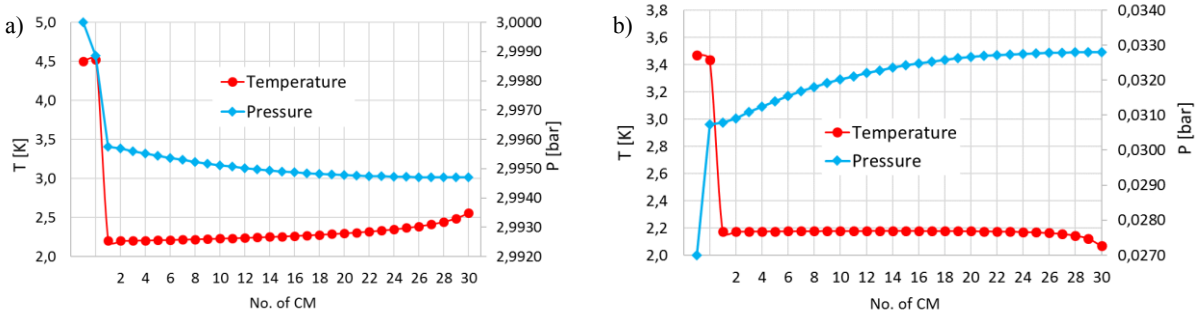

Figure 4. Distributions of temperature, pressure along the He supply (a) and VLP return (b) lines for Layout 2 in Configuration 1 and subjected to HL3

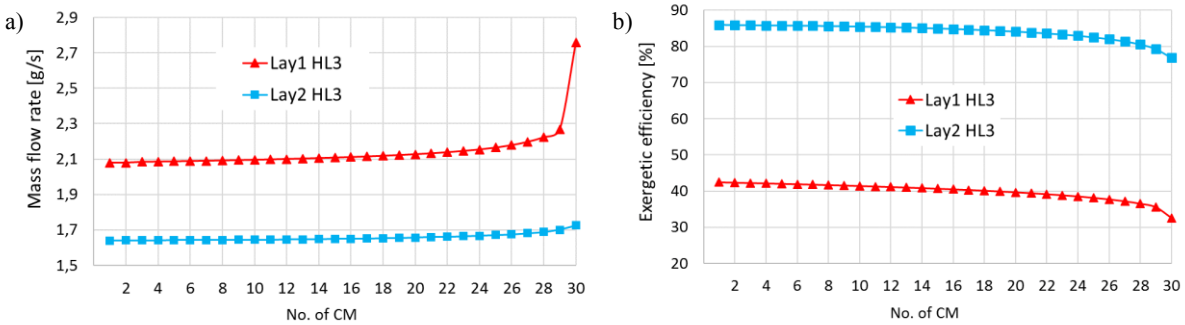

Figure 5. Distributions of mass flow rate (a) in CMs and their exergetic efficiencies (b)

The total exergetic efficiency of Layout 1 is in the range of 55% to 47% and for Layout 2 between 65% and 54% for the analyzed configurations and heat load cases (refer to Figure 6). Such higher

efficiencies of Layout 2 result from smaller thermal losses in the main circuit (He supply and VLP line). In the analyzed distribution systems these thermal losses are the main sources of irreversible processes.

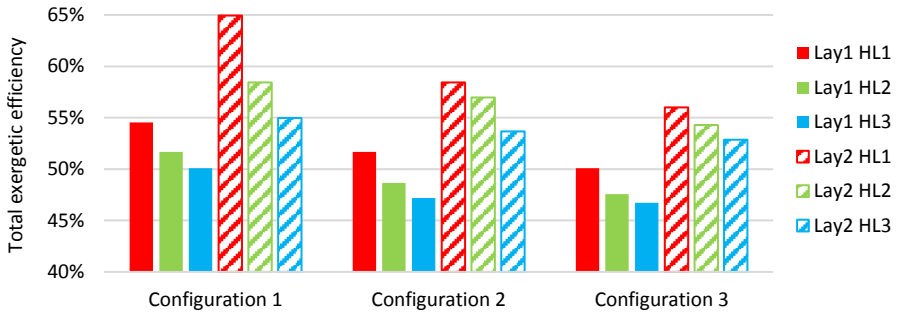

Figure 6. Total exergetic efficiency in respect to heat loads and configurations of helium distribution systems in Layouts 1 and 2

4. Conclusions

For input data given in Tables 1 and 2 the distribution system with one central heat exchanger (Layout 2) is characterized by higher total exergetic efficiency. The difference varies from 5 to 10% and strongly depends on heat loads and geometrical configurations (see Figure 6). According to its definition, the exergetic efficiency shows how far (or close) a system is from the Carnot reversed cycle which is an ideal reversible refrigerator with η_{ex} = 100%. For real cryogenic systems, the lower the exergetic efficiency is the more irreversible losses are in the system and in consequence a higher cooling power is required to be provided from the cryoplant. A difference of 5-10% shows that Layout 2 is significantly more efficient than Layout 1. It can be directly converted to work that needs to be delivered to the system in order to obtain the required cooling effect. In case of the highest difference (10% for HL1), the real and useful works for Layout 1 are 183.2 kW and 99.9 kW, whist for Layout 2 only 117.9 kW and 76.6 kW, respectively. Layout 2 requires considerably less real work and the use of this work is much more effective.

Results of such analyses can be very useful in selection of the most appropriate layout for any cryogenic installations. However, since they refer to the operational cost only, they must be supported by detailed analyses of total capital costs including investment and maintenance costs.

References

[1] Erdt. W. et al. The cryogenic distribution line for the LHC: functional specification and conceptual design, LHC Project Report 326, 1999, p. 8
[2] Arenius D. et al. Cryogenic System for the Spallation Neutron Source, Transactions of the Cryogenic Engineering Conference – CEC, Vol 49, 2004, pp. 200-2007
[3] Fydrych J. et al. Cryogenic Distribution System for the ESS Superconducting Proton Linac, Physics Procedia 67, 201, pp. 828 – 833
[4] The PIP-II Conceptual Design Report, Edited by Valeri Lebedev, Section 3.4.3 The Cryogenic Distribution System, 2017, pp. 187-189
[5] Lierl H. et al. Conceptual layout of the european x-fel linear accelerator cryogenic supply, Proceedings of LINAC 2004, Lübeck, Germany, 2004, pp. 225-227
[6] Dalesandro A. et al. Thermodynamic Analyses of the LCLS-II Cryogenic Distribution System IEEE Transactions on Applied Superconductivity, Vol. 27, No. 4, 2017, Sequence #: 0500804
[7] Ziegler B.O. Second law analysis of the helium refrigerators for the HERA proton magnet ring, Advances in Cryogenic Engineering, 1986, pp. 693-698
[8] Claudet S. et. al. Exergy analysis of the cryogenic helium distribution system for the Large Helium Collider (LHC), Transactions of the Cryogenic Engineering Conference – CEC, Vol 1218, 2010, pp. 1267-1274